

Production and Characterization of Blow-Spun Recycled Polycarbonate Nanofibers Using the Airbrush System

Filipe de Almeida Araújo^{a*} , Antônio Augusto Martins Pereira Junior^b , Ricardo Pondé Weber^c 

^aUniversidade Federal de São Carlos (UFSCar), Departamento de Engenharia de Materiais (DEMA), São Carlos, SP, Brasil.

^bUniversidade Federal do Rio de Janeiro (UFRJ), Parque Tecnológico, Rio de Janeiro, RJ, Brasil.

^cInstituto Militar de Engenharia (IME), Departamento de Ciências de Materiais, Rio de Janeiro, RJ, Brasil.

Received: January 14, 2023; Revised: April 10, 2023; Accepted: May 21, 2023

This paper evaluates the use of the airbrush adapted solution blow spinning process as a secondary recycling method to produce recycled polycarbonate nanofibers. The results show a gradual improvement in fiber morphology and reduction in fiber diameter with increasing concentration, obtaining fibers at 18% w/v, indicating that the process is effective in producing high-quality nanofibers. The ideal morphology for the samples was obtained under 21%w/v and 60 Psi of air pressure with an 80nm average diameter. The thermal analysis demonstrates that the fibers possess similar thermal behavior to pure polycarbonate while the oxidation index didn't show significant degradation on the fibers, suggesting that they can be used as standalone nanofibers for advanced applications. The produced nanofibers have diameters below 100 nm, making them suitable for use in face mask filters, among other applications. The study provides a new approach for the recycling of polycarbonate materials, offering a sustainable solution for their reuse.

Keywords: *nanofibers. polycarbonate. solution blow spinning. recycling*

1. Introduction

During the coronavirus pandemic, diverse industry sectors have faced multiple challenges. One of the most affected areas was the Personal Protective Equipment (PPE) sector due to the huge demand for masks and face shields, which caused a shortage of polymeric material worldwide as well as a scarcity of masks with proper filtration capacities in hospitals¹⁻³.

Mask filters are often composed from layers of microfibers; however, nanofibers could be seen as potential substitutes for such microfibers used in masks and respirators due to their better properties². Nanofibers display higher surface area, uniform morphology and higher cytocompatibility than microfibers, without presenting deleterious effects on the organism^{2,4}. They are defined as fibers with a diameter in the nanoscale which can be obtained from polymer solutions or melts.

Common nanofiber production methods are classified as electrospinning and blow spinning, each possessing advantages and disadvantages. Electrospinning is widely used and reported in the literature for nanofiber production. This process is based on the application of electrostatic forces, obtaining fibers with diverse diameters and morphology⁵⁻¹¹.

The blow spinning technique reported by Medeiros et al.¹² makes use of a pump and a syringe through which a polymer solution is pumped through a nozzle system. This system consists of a set of concentric nozzles where the solution flows through the inner nozzle while a high velocity gas is

pumped on the outer nozzle spraying the solution towards a collector plate¹³⁻¹⁷.

Polycarbonates are thermoplastic polymers synthesized by condensation, widely used in injection molding due to their physical and mechanical properties, possessing heat resistance and ductility on impact giving it the name "engineering material", allowing the application in multiple sectors in which can be highlighted the, automotive, electronics and health sectors^{3,18-22}.

The usage of polymers brings out particularities regarding their disposal and recycling, which have been elated over the past years. Standard polymer waste treatments employed such as incineration and landfill are not environmentally sustainable. One of the most common options to circumvent this issue is the use of recycling via mechanical grinding and reprocessing by extrusion, however this method results in negative changes on the polymer properties due to thermal aging^{23,24}.

Polycarbonate solutions have been previously reported on the production of nanofibers using electrospinning^{25,26}, and the production of nanofibers using recycled materials has been possible with the melt spinning process with commercial scale^{3,27,28}.

The blow spinning technique can be a new method for producing nanostructured materials using waste, as this methodology presents multiple advantages regarding the production of polymeric nanomaterials. These include ease of construction and installation of the devices and equipment used in production, a higher deposition rate, and a wider

*e-mail: filipe.almeida.araujo@gmail.com

range of polymer types that can be used when compared to melt and electrospinning^{3,7}.

The study aimed to expand the technological horizon presenting innovations regarding the processing of polycarbonate waste, using solution blow spinning to produce recycled non-woven nanofibers as a secondary recycling method. Additionally, the research focused on the characterization of the produced material, with a particular emphasis on the analysis of morphological aspects, dimensional parameters of the nanofibers, and thermal and degradation analysis.

2. Materials and Methods

2.1. Processing

Polycarbonate samples used in this study were obtained as industrial waste from an injection molding process, being polymers that remained in the machine post processing. The samples belonged to the MaKrolon® brand and were donated by the company WS Moldes localized within Rio de Janeiro. The solvent used was a Chloroform P.A.ACS, as it displayed the best solubilization time for polycarbonate, and its high volatility allowed it to evaporate during the blowing process. All polymer solutions were prepared under constant magnetic stirring for 1 hour at 25 °C.

The blow spinning system used in this study was built from scratch inside the institute's polymer testing laboratory, where it was conceived, starting from the compatibility of a double action airbrush with concentric nozzles (inner and outer nozzle). As mentioned previously, the inner nozzle controls the solution flux and the outer one where the pressurized gas flows. The layout was composed of a gas pump, airbrush and a rotatory collector plate set at 20 rpm as illustrated in Figure 1. Unlike traditional blow spinning methods, the airbrush system used in this study requires trial and error to determine the optimal solution concentration. Too high a concentration can cause the airbrush to clog, while too low a concentration can prevent fiber formation, meaning lesser control of flow rate which varies with solution viscosity. However, the portability of this system allows for in situ deposition of nanofibers by hand, unlike electrospinning, as the position used will not affect fiber formation. Overall, the system used in this study offers a method for producing

nanofibers from polycarbonate waste, with the potential to be applied to other types of waste polymer materials²⁹⁻³¹.

For determination of max sample size an experimental design was used, the analysis used polymer solution concentration and work pressure as the variables since previous research points them as factors which display higher influence in fiber morphology^{6,10,16}. The analysis was conducted using the R® software, where it was possible to establish inherent conditions for the study. As such it was established as a factorial 9x2 with 3 repetitions, obtaining in total 18 samples. This allowed for a systematic investigation of the effects of different combinations of polymer solution concentration and work pressure on the resulting nanofibers.

The process was initiated by cleaning and drying of the polycarbonate waste for removal of impurities followed by solubilization using chloroform in solutions ranging from 10%, 12%, 15%, 16%, 17%, 18%, 19%, 20% and 21% w/v of polycarbonate. The use of chloroform comes from its high volatility which facilitates solvent evaporation during the process, NMP and THF were also tested as possible solvents but were unable to solubilize PC in concentrations above 10%w/v³.

Following the previous step, the solutions were taken to the reservoir in the airbrush for blow spinning with air pressure varying between 40psi and 60psi. The following process conditions were used: inner nozzle diameter of 0,3mm, distance to collector of 30 cm, deposition on aluminum sheets and ambient process conditions with a temperature of 25 °C and relative humidity of about 55%.

2.2. Characterization

Initially, a dimensional and morphological characterization of samples for the selection of ideal parameters was performed using Scanning Electron Microscopy (SEM). Next the samples were submitted to the processes of physical and chemical characterization with Fourier Transform Infrared Spectroscopy (FTIR), Differential Scanning Calorimetry (DSC), Thermogravimetric Analysis (TGA) and Gel Permeation Chromatography (GPC).

To quantify fiber diameter size and morphology evolution with increase of solution diameter concentration the sample's morphology was analyzed by Scanning Electron Microscopy (SEM), under increasing magnification, using a beam varying between 1 to 30kV with a Quanta FEG 250 FEI microscope; sample preparation consisted of gold coating prior to the testing.

The Fourier Transformed Infrared Spectroscopy (FTIR) was tested within the wavelength region of 400cm⁻¹ to 4000cm⁻¹. The transmission spectrum was obtained in a resolution of 4cm⁻¹ with 64 scans per test using a spectrometer model Thermo Scientific Nicolet iS10. After analysis, the oxidation index was calculated to identify breakage on the main polymer chains, using the carbonyl absorption peaks (1775cm⁻¹) and the intensity of the peak in 760cm⁻¹, according to the Equation 1³².

$$IO = I(1775) / I(760) \quad (1)$$

To determine the thermal properties of the obtained nanofibers, a thermogravimetric analysis was applied to the

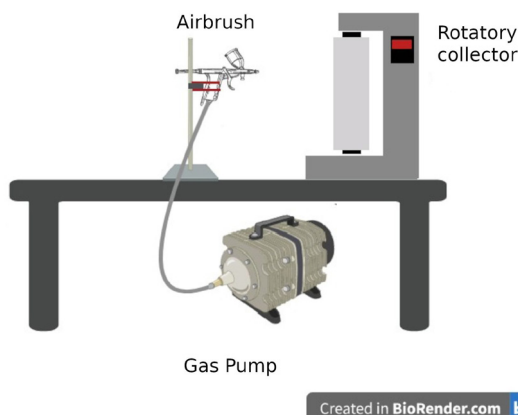


Figure 1. Illustration of the solution blow spinning system.

base material and nanofiber samples following the premises established by the ASTM E1131³³. The equipment used was the TA instruments thermogravimetric analyzer model TGA Q500, the procedure submitted samples (5mg) to a heating cycle up to 700°C under a heating rate of 10°C/min³².

The characterization by Differential Scanning Calorimetry (DSC) was done using a DSC Q1000 machine and followed the specifications within the ASTM D3418³⁴ standard. The technique was used to observe any changes of properties between the samples and the base material, for which a heat cycle was applied from 25°C up to 300°C at a rate of 10 °C/min. To identify the molecular weight of the samples and ascertain possible degradation effects the GPC technique was used, following the ISO 13885³⁵ using Prominence UFLC equipment.

3. Results and Discussion

3.1. Morphology characterization by Scanning Electron Microscopy

The analysis on the influence of the work parameters and boundary conditions applied in the process of nanofiber production was investigated via SEM. Therefore, starting from

10% w/v concentration the samples revealed a morphology with high concentration of polymer agglomerates and beads. Upon an increase of concentration up to 15%w/v (Figure 2) the formation of fibers was observed, with a medium diameter of 1,18µm. It was noted that the samples in this group displayed similar behavior in both 40 Psi and 60 Psi work pressure. As such the morphology obtained on the samples on Figure 2 suggests the solution have not yet reached its overlap concentration.

It is important to note that the fiber morphology on the airbrush system is dependent on the overlap concentration and viscosity of the solution, given the feed rate is gravity controlled, instead of a syringe pump for feed control as normal blow spinning uses. The literature however suggests these effects cannot be directly correlated to one another as each system uses different parameters while reaching identical structures^{29,30}.

At concentrations of 16% w/v and 17% w/v (Figure 3), the polymer agglomerates were reduced in quantity and size, and the fiber diameter was further reduced. These changes in morphology suggest that the polymer chains are more entangled, allowing for the formation of thinner fibers and reducing the occurrence of beads and agglomerates. These observations highlight the importance of solution concentration in controlling the morphology of the produced fibers.

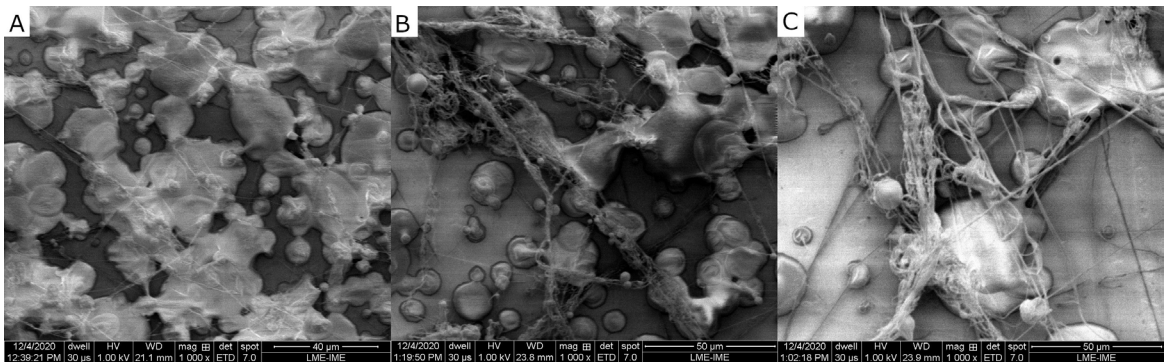


Figure 2. Morphology of the samples obtained from concentrations of: (A)10%, (B)12%, and (C)15%w/v. With work pressure of 40 Psi and 60 Psi and distance of 30 cm.

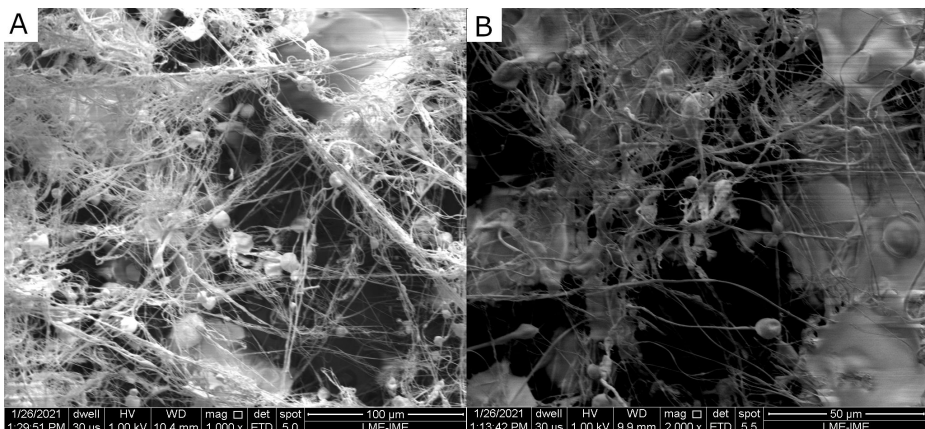


Figure 3. Morphology of the samples obtained from concentrations of: (A)1000x 16%w/v and (B) 2000x 17%w/v. With work pressure of 40 Psi and 60 Psi and distance of 30 cm.

It is also observed the formation of beads on a string morphology as an indication that the solution is approaching the overlap concentration, which is the concentration where the individual polymer chains in the solution start to entangle with each other, forming a network that can support the formation of continuous fibers.

Starting at 18% w/v, the viscosity of the solution became too high to pass through the nozzle with 40psi of work pressure. Therefore, the remaining samples were processed with 60psi only. The SEM analysis on the following samples used varying magnification in order to have a better view on the fiber mats and fiber diameter. The samples analyzed under 1000x magnification show a significant reduction in bead and polymer agglomerate presence when compared to lower concentrations. The reduction in bead and polymer agglomerate presence at higher concentrations suggests that the overlap concentration was reached. The medium diameter for fibers appearing in the range of 800 nm (Figure 4B) further confirms that the samples reached the overlap concentration, validating the effectiveness of the blow spinning process for polycarbonate nanofiber production at high concentrations³.

The airbrush technique is known to produce a high presence of beads and fiber bundles compared to normal blow spinning, as reported in the literature. However, at high polymer concentrations, it is possible to significantly reduce the occurrence of these defects, resulting in fibrous scaffolds with highly localized alignment or multiple fiber strands or bundles. This behavior is challenging to obtain using other methods like electrospinning^{29-31,36}. As such, further increments in concentration were tested to reach this optimum state of the fiber mats.

With another increment in concentration to 19% w/v, it is observed in the 15,000x magnification (Figure 5A) the presence of non-woven fibers endowed with randomized dispersion. Within a 50,000x magnification (Figure 5B) the medium fiber diameter observed was in the 150 nm range. Additionally, fibers with diameters below 100 nm were observed in the micrographs presented. At 20% w/v, the samples exhibited similar behavior, producing diameters below 100 nm, as shown in the 5,000x magnification, without the presence of other morphologies. Figure 5 presents the

morphologies of the samples from 19% w/v to 20% w/v, respectively.

The samples produced with a concentration of 21% w/v show similar morphology to those produced with a concentration of 20% w/v. Both concentrations were processed with an average flow rate of 0.25 ml/min, resulting in the production of fibers with small diameters without the presence of beads and agglomerates. The fibers obtained in this concentration (Figure 6) showed a higher alignment of its bundles compared to the previous samples which is in accord to airbrushed highly concentrated polymer solutions using elevated air pressure^{29,31}.

According to Figure 7, it is observed a reduction on the medium fiber diameter (80nm) at 50,000x. Upon verifying these dimensional parameters, it is attested the produced materials are classified on the 1-D nanomaterial dimensionality^{30,31}.

The box plot presents the range of distribution from the samples produced at 60 Psi. Based on the results shown in Figure 8, it can be noted that an increase in solution concentration (19%-21%w/v) leads to a reduction in the diameter of the samples. The overall sample morphologies can be related to the four regimes of polymer chain overlap, which are described as: dilute, semidilute-unentangled, semidilute-entangled and concentrated. The first point of transition is observed at 15%w/v with the formation of beaded fibers, indicating a transition from a diluted solution into a semidilute regime³⁰. A second point of transition is observed at 20%w/v, where a significant portion of the bead morphology is stretched into fibers, representing the transition to a concentrated regime.

The average fiber diameter obtained in this study allows for the potential use of the fiber mats in various applications. For example, typical facemask filters have a diameter range of approximately 12 to 20 μm , while N95 respirators have a diameter range of approximately 2 to 7 μm ^{37,38}. In recent years, the COVID-19 pandemic has led to increased research and use of ultrafine fibers as intermediary filters, due to their high surface-to-volume ratio, diverse surface chemistry, and ability to form a high and interconnected porosity, resulting in advanced face masks³⁷. Recycled nanofibers have also been pointed as potential filters for wastewater treatment however they face challenges due their low mechanical strength³⁹⁻⁴¹.

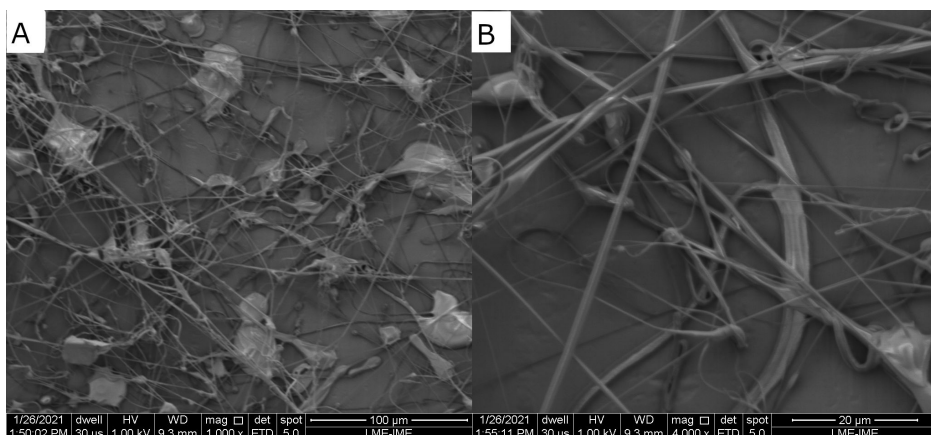


Figure 4. Morphology of the samples obtained from concentrations of: (A) 1000x 18%w/v and (B) 4000x 18%w/v. With work pressure of 60 Psi and distance of 30 cm.

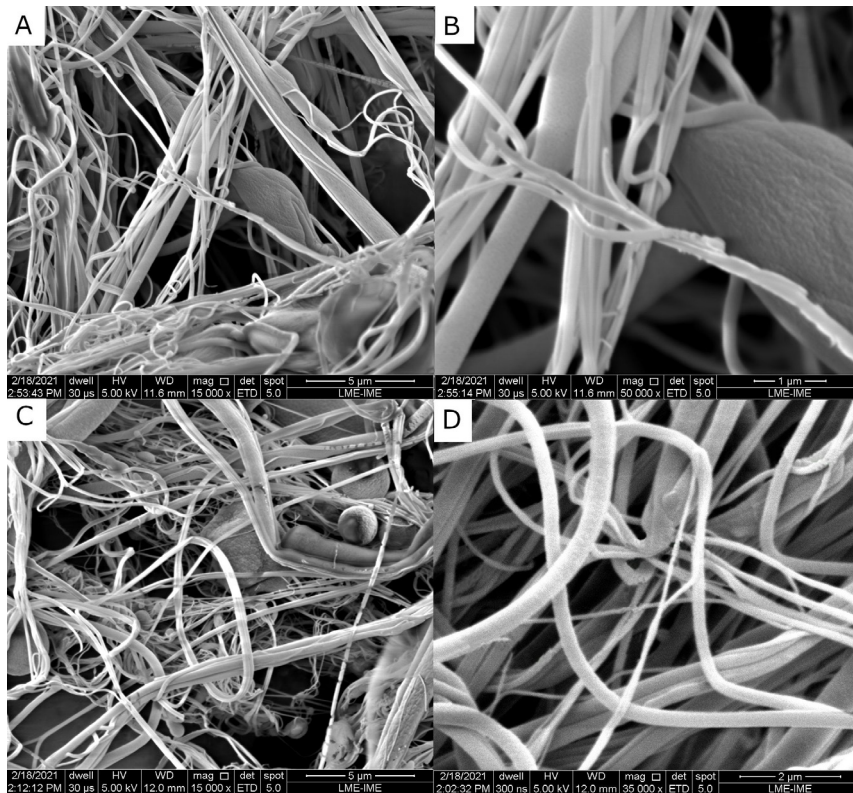


Figure 5. Morphology of the samples obtained from concentrations of: (A) 15000x 19%w/v, (B) 50000 19%w/v, (C) 20000x 20%w/v and (D)35000x 20%w/v. With work pressure of 60 Psi and distance of 30 cm.

3.2. Fourier Transformed Infrared Spectroscopy (FTIR)

The FTIR spectra of the samples were compared to the base material as presented on Figure 9. It's important to showcase that the analysis was centered only on the samples with concentration ranging from 19%w/v to 21%w/v, as they displayed the adequate morphologies. Given this, the sample characterization used a new notation: 19%NF, 20%NF and 21%NF.

On the transmittance bands are observed the characteristic peaks of the polycarbonate (PC) relative to the vibrational points of C-H bounds (2975cm^{-1}), carbonyl stretching (1755cm^{-1}), C-O bonds (1227cm^{-1}) and aromatic ring stretching (1500cm^{-1})^{22,32,41-45}.

Due to the shear effect on the solution caused by the high air pressure during the spraying, an oxidation index (OI) analysis was used to verify possible degradation effects that may occur during the blow spinning. Table 1 shows the degradation values obtained by the OI, where it is observed the samples did not display significant variation on its oxidation value when compared to the polycarbonate as received, demonstrating no polymer chain scission happened during the process.

3.3. Thermogravimetric Analysis (TGA)

The thermograms displaying the characteristic curves for the nanofiber samples ranging from 19% w/v to 21% w/v and polycarbonate in its received state (PC) are presented

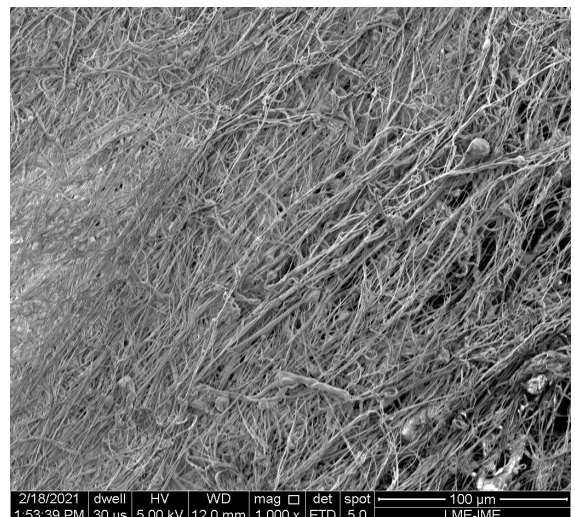


Figure 6. General morphology of the fiber mats obtained from concentrations of 21%w/v. With work pressure of 60 Psi and distance of 30 cm.

in Figure 10. Based on previous studies, the behavior of the processed samples closely resembles that of pure PC (unprocessed), thus exhibiting a single step decomposition that begins at 430°C and ends at 550°C ^{45,46}.

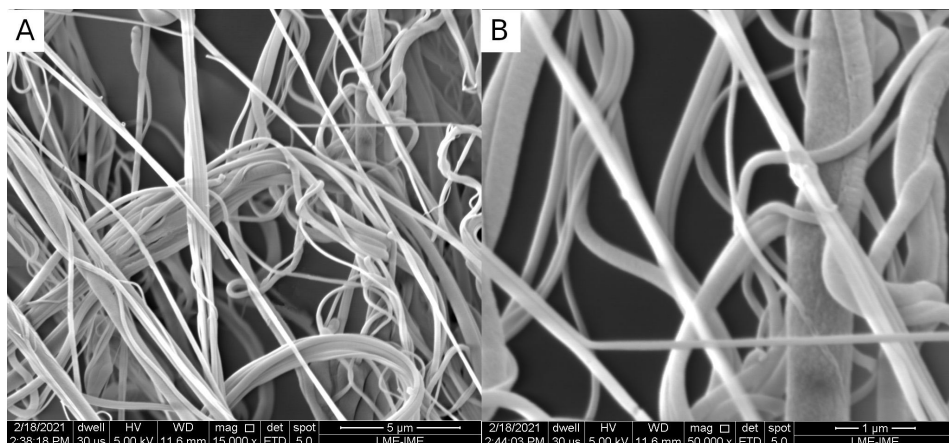


Figure 7. Morphology of the samples obtained from concentrations of 21%w/v. With work pressure of 60 Psi and distance of 30 cm.

Table 1. Oxidation index values for the nanofiber samples and polycarbonate as received.

Sample	Index (1775)
OI PC	0.98
OI PC NF 19% w/v	0.95
OI PC NF 20% w/v	0.96
OI PC NF 21% w/v	0.94

The 19%w/v sample has its respective T_{onset} beginning at 435.91°C, the 20%w/v and 21% w/v samples have their T_{onset} at 430.00°C and 436.11°C.

The polycarbonate as received presented a T_{onset} at 458,90°C which can indicate a stronger thermal stability when compared to the nanofiber samples, this difference could be related to the internal stress on the fibers caused by the blow spinning.

3.4. Differential scanning calorimetry (DSC)

Polycarbonates possess a particular behavior, despite being an amorphous polymer they can crystallize when subjected to a solubilization process, as observed in several studies⁴⁷⁻⁴⁹. Solubilization is a part of the solution blow spinning process. Therefore, the effects of solubilization on the samples were analyzed using DSC with two heating runs, as crystallization peaks can be detected during the first heating cycle of DSC.

The first and second heating run curves of the 3 main nanofiber samples can be seen on Figure 11, it is observed a slight rise in the glass transition temperature from 140°C to 143°C according to the increasing solution concentration used, effect that may be related to the polymer chain orientation during the stretching caused by the process¹².

Within the equipment sensibility, no crystallinity peaks were observed at the temperatures indicated by the literature on the nanofiber samples, concluding that even though the process is solubilizing the polycarbonate, the fibers are not presenting crystallinity.

Observing the second run curves, we can evaluate the samples post a tempering process, the samples show a glass transition (T_g) around 140°C for the 3 samples. As such the

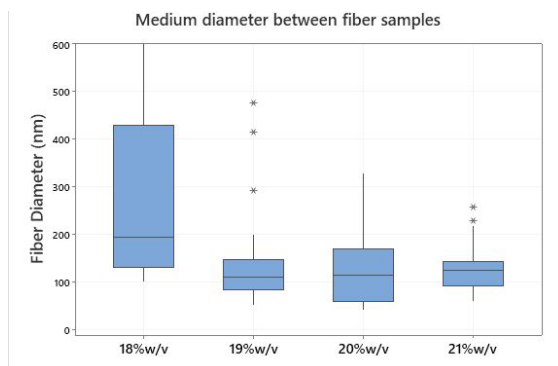


Figure 8. Samples medium diameter range from 18%w/v to 21%w/v at 60 Psi.

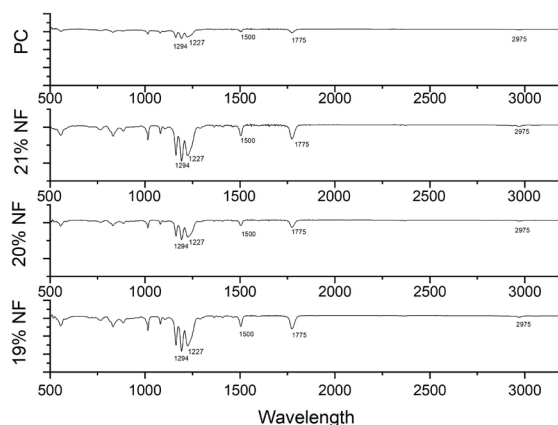


Figure 9. Transmission spectra of samples with 19%w/v to 21%w/v.

macromolecules did not show signs of thermal degradation with its transition temperatures under the experimental error.

The DSC curves for the solubilized polycarbonate and the polycarbonate as received are shown in Figure 12, the samples demonstrate the standard polycarbonate glass transition temperature according to the literature at 148°C.

It's also observed the crystallinity peaks between 220 and 230°C on the solubilized polycarbonate^{49,50}.

The relative crystallization percentage was calculated using the equilibrium enthalpy for the solubilized polycarbonate ($\Delta H^0 = 110.0\text{J/g}$), obtaining a value of 77% which disappears after the second heating cycle, the lack of crystallinity peaks

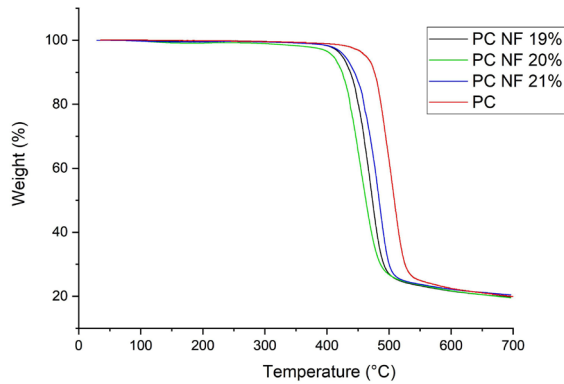


Figure 10. Comparative thermogram of the samples with the polycarbonate as received.

on the fiber samples shows that the blow spinning processing kept the fibers with a predominantly amorphous behavior⁵¹.

Nanofiber processing using polycarbonate can vary the fibers thermal properties with a rise in the T_g (glass transition) value as reported by other solution-based processes^{11,42}. The samples studied did not display such behavior, the slight variations found on the DSC and TGA values can be related to the high shear strength on extrusion-based processes like melt spinning and blow spinning, however no chain scission effects were observed⁵⁰. Those results suggest that fibers have not suffered significant loss on its properties despite being waste material, allowing them the same practical uses where neat polycarbonate nanofibers would be used.

3.4. Gel Permeation Chromatography (GPC)

GPC analyses were performed on samples of the PC as received and nanofibers produced under 21%w/v, Figure 13 shows the curves obtained for the materials, where a similar behavior is found between both. The values of molecular weight (M_w) for the polycarbonate as received (PC) were 55481 and 53512 for the fiber sample (PCNF 21%). These values confirm that no significant chain scission was caused on the macromolecules of the fibers by the blow spinning processing.

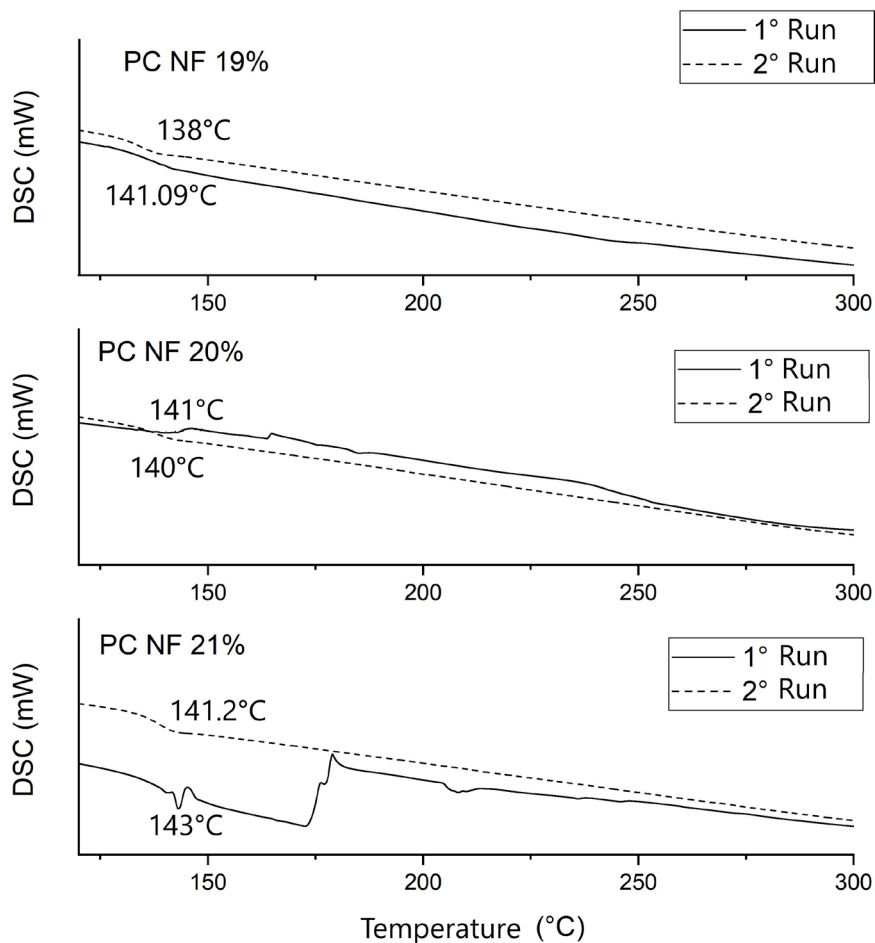


Figure 11. DSC curves for the nanofiber samples from 19%w/v to 21%w/v under 2 heating runs.

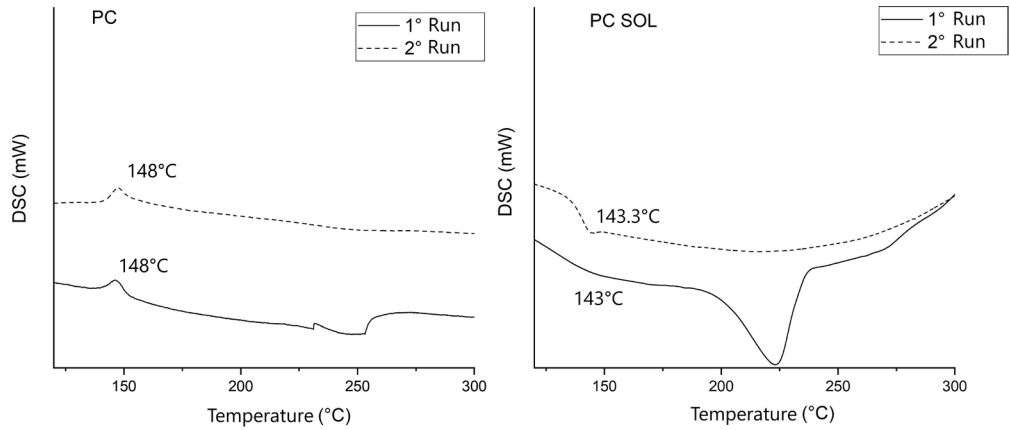


Figure 12. DSC curves for the polycarbonate as received (PC) and solubilized (PC SOL) under 2 heating runs.

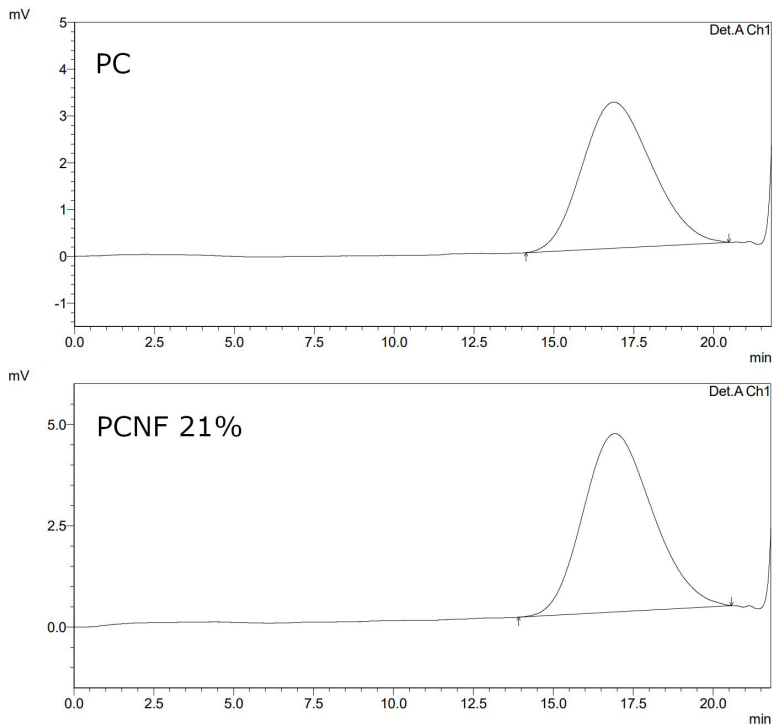


Figure 13. GPC curve for the polycarbonate as received (PC) and nanofiber produced with 21%w/v (PCNF 21%).

4. Conclusions

The production of recycled polycarbonate nanofibers using the airbrush adapted solution blow spinning system was reported in the present study. With observance to the morphology on the SEM images, the production of nanofibers was evidenced starting at 18%w/v.

The presented results demonstrate the adequacy of the airbrush adapted solution blow spinning technique to produce nanofibers. In comparison to other techniques such as electrospinning that uses high voltage and melt spinning that

uses temperature, this technique is more economical and easier to install and operate. These advantages make it a promising option for commercial scale production of nanofibers.

Between the concentrations of 20% and 21% w/v, the fibers obtained exhibit a non-woven morphology without the presence of other structures such as agglomerates or beads-on-a-string with an average diameter of 80nm. Based on the FTIR results, the processing of the fibers did not cause significant variations in the chemical bonds of the polycarbonate, nor did it indicate any oxidation effects related to scission of the main polymer chains.

The thermogravimetric analysis has shown the fibers have a similar thermal behavior to neat polycarbonate, showing similar thermal stability to the fibers. The curves obtained from the DSC, show values for T_g of 140°C to 143°C, corresponding to the values of the polycarbonate as received.

The nanofibers did not present peaks related to crystallization effects post solubilization which occur in polycarbonates. This information indicates that the fibers produced with solution blow spinning maintain their predominantly amorphous behavior. Within the experimental data, the samples with 21%w/v and 60 Psi presented the better thermal properties and morphology evidencing the potential of this nanomaterial in many industrial applications, such as filters and masks.

For future research, it would be valuable to investigate the impact of solution viscoelasticity on the morphological properties of the fibers to enable better control of stretchability during processing. Additionally, exploring the filtration capabilities of the fibers for potential applications in face masks, as well as conducting mechanical testing, would be interesting avenues of research.

5. Acknowledgments

The authors of this article thank the Brazilian support agencies Coordination for the Improvement of Higher Education Personnel (CAPES) and the National Council for Scientific and Technological Development (CNPq) for the support.

6. References

1. Wu H-L, Huang J, Zhang CJP, He Z, Ming W-K. Facemask shortage and the novel coronavirus disease (covid-19) outbreak: reflections on public health measures. *EClinicalMedicine*. 2020;21:100329. <http://dx.doi.org/10.1016/j.eclim.2020.100329>.
2. Ullah S, Ullah A, Lee J, Jeong Y, Hashmi M, Zhu C, et al. Reusability comparison of melt-blown vs nanofiber face mask filters for use in the coronavirus pandemic. *ACS Appl Nano Mater*. 2020;3(7):7231-41. <http://dx.doi.org/10.1021/acsnano.0c01562>.
3. Araújo FA, Pereira AAM Jr, Weber RP. Production of a recycled polycarbonate nanofiber using the blow-spinning process. In: *CBEiMat*; 2022 Nov 6-10; São Paulo. São Carlos: UFSCar; 2022. p. 873-1.
4. Sousa MG, Rezende TM, Franco OL. Nanofibers as drug-delivery systems for antimicrobial peptides. *Drug Discov Today*. 2021;26(8):2064-74. <http://dx.doi.org/10.1016/j.drudis.2021.03.008>. PMID:33741497.
5. Luraghi A, Peri F, Moroni L. Electrospinning for drug delivery applications: a review. *J Control Release*. 2021;334:463-84. <http://dx.doi.org/10.1016/j.jconrel.2021.03.033>. PMID:33781809.
6. Oliveira JE, Mattoso LHC, Orts WJ, Medeiros ES. Structural and morphological characterization of micro and nanofibers produced by electrospinning and solution blow spinning: a comparative study. *Adv Mater Sci Eng*. 2013;2013:1-14. <http://dx.doi.org/10.1155/2013/409572>.
7. Dadol GC, Kilic A, Tijing LD, Lim KJA, Cabatingan LK, Tan NPB, et al. Solution blow spinning (SBS) and SBS-spun nanofibers: materials, methods, and applications. *Mater Today Commun*. 2020;25:101656. <http://dx.doi.org/10.1016/j.mtcomm.2020.101656>.
8. Daristotle JL, Behrens AM, Sandlerand AD, Kofinas P. A review of the fundamental principles and applications of solution blow spinning. *ACS Appl Mater Interfaces*. 2016;8(51):34951-63. <http://dx.doi.org/10.1021/acsami.6b12994>. PMID:27966857.
9. Dayong Y, Yang W, Dongzhou Z, Yingyi L, Xingyu J. Control of the morphology of micro/nano- structures of polycarbonate via electrospinning. *Chin Sci Bull*. 2009;54:2911-7. <http://dx.doi.org/10.1016/j.eclim.2020.100329>.
10. dos Santos DM, Correa DS, Medeiros ES, Oliveira JE, Mattoso LHC. Advances in functional polymer nanofibers: from spinning fabrication techniques to recent biomedical applications. *ACS Appl Mater Interfaces*. 2020;12(41):45673-701. <http://dx.doi.org/10.1021/acsami.0c12410>. PMID:32937068.
11. Dhakate S, Singla B, Uppal M, Mathur R. Effect of processing parameters on morphology and thermal properties of electrospun polycarbonate nanofiber. *Adv Mater Lett*. 2010;1(3):200-4. <http://dx.doi.org/10.5185/amlett.2010.8148>.
12. Medeiros ES, Glenn GM, Klamczynski AP, Orts WJ, Mattoso LHC. Solution blow spinning: a new method to produce micro- and nanofibers from polymer solutions. *J Appl Polym Sci*. 2010;113(4):2322-30.
13. Anstey A, Chang E, Kim ES, Risvi A, Kakroodi AR, Park CB, et al. Nanofibrillated polymer systems: design, application, and current state of the art. *Prog Polym Sci*. 2021;113:101346.
14. Zhuang X, Jia K, Cheng B, Feng X, Shi S, Zhang B. Solution blowing of continuous carbon nanofiber yarn and its electrochemical performance for supercapacitor. *Chem Eng J*. 2014;237:308-11. <http://dx.doi.org/10.1016/j.cej.2013.10.038>.
15. Song J, Li Z, Wu H. Blowspinning: a new choice for nanofibers. *ACS Appl Mater Interfaces*. 2020;12(30):33447-64. <http://dx.doi.org/10.1021/acsami.0c05740>. PMID:32628010.
16. Sinha-Ray S, Sinha-Ray S, Yarin AL, Pourdeyhimi B. Theoretical and experimental investigation of physical mechanisms responsible for polymer nanofiber formation in solution blowing. *Polymer (Guildf)*. 2015;56:452-63. <http://dx.doi.org/10.1016/j.polymer.2014.11.019>.
17. Li R, Li Z, Yang R, Yin X, Lv J, Zhu L, et al. Polycaprolactone/poly(l-lactic acid) composite micro/nanofibrous membrane prepared through solution blowspinning for oil adsorption. *Mater Chem Phys*. 2020;241:122338. <http://dx.doi.org/10.1016/j.matchemphys.2019.122338>.
18. Ebeuwele RO. *Polymer science and technology*. 1st ed. New York: CRC Press; 2000. <http://dx.doi.org/10.1201/9781420057805>.
19. Legrand DG, Bendler JT. *Handbook of polycarbonate science and technology*. 1st ed. New York: Marcel Dekker; 2000. 531 p.
20. Kutz M. *Applied plastics engineering handbook*. 2nd ed. United Kingdom: Elsevier; 2017.
21. Mano EB, Mendes CL. *Introdução a polímeros*. 2. ed. United Kingdom: Edgard Blucher; 2004. 191 p.
22. Zhang W, Xu Y. *Mechanical properties of polycarbonate: experiment and modeling for aeronautical and aerospace applications*. 1st ed. United Kingdom: Elsevier; 2019. 186 p.
23. Wu CH, Chen L-Y, Jeng R-J, Dai SA. 100% atom-economy efficiency of recycling polycarbonate into versatile intermediates. *ACS Sustain Chem& Eng*. 2018;6(7):8964-75. <http://dx.doi.org/10.1021/acssuschemeng.8b01326>.
24. Antonakou EV, Achilias DS. Recent advances in polycarbonate recycling: a review of degradation methods and their mechanisms. *Waste Biomass Valoriz*. 2013;4(1):9-21. <http://dx.doi.org/10.1007/s12649-012-9159-x>.
25. Hsiao H-Y, Huang C-M, Liu Y-Y, Kuo Y-C, Chen H. Effect of air blowing on the morphology and nanofiber properties of blowing-assisted electrospun polycarbonates. *J Appl Polym Sci*. 2010;124(6):4904-14.
26. Yang D, Wang Y, Zhang D, Liu Y, Jiang X. Control of the morphology of micro/nano- structures of polycarbonate via electrospinning. *Chin Sci Bull*. 2009;54:2911-7.
27. Tuladhar R, Yin S. Production of recycled polypropylene (PP) fibers from industrial plastic waste through melt spinning process. In: Pacheco-Torgal F, Khatib J, Colangelo F, Tuladhar

- R. Use of recycled plastics in eco-efficient concrete. Sawston, Reino Unido: Woodhead Publishing; 2019. p. 69-84.
28. Santos RPO, Ramos LA, Frollini E. Bio-based electrospun mats composed of aligned and nonaligned fibers from cellulose nanocrystals, castor oil, and recycled pet. *Int J Biol Macromol*. 2020;163:878-87. <http://dx.doi.org/10.1016/j.ijbiomac.2020.07.064>. PMID:32653368.
 29. Hell AF, Simbara MM, Rodrigues P, Kakazu DA, Malmonge SM. Production of fibrous polymer scaffolds for tissue engineering using an automated solution blow spinning system. *Res Biomed Eng*. 2018
 30. Dias FT, Rempel SP, Agnol LD, Bianchi O. The main blow spun polymer systems: processing conditions and applications. *J Polym Res*. 2020;27:205.
 31. Dias GC, Cellet TS, Santos MC, Sanches AO, Malmonge LF. PVDF nanofibers obtained by solution blow spinning with use of a commercial airbrush. *J Polym Res*. 2019;26(4):87.
 32. Weber R. *Influência do envelhecimento no comportamento dinâmico do policarbonato*. Rio de Janeiro: Instituto Militar de Engenharia; 2010. 128 p.
 33. ASTM: American Society for Testing and Materials. ASTM E1131-20: standard test method for compositional analysis by thermogravimetry. West Conshohocken, PA: ASTM International; 2020. p. 6. <http://dx.doi.org/10.1520/E1131-20>.
 34. ASTM: American Society for Testing and Materials. ASTM D3418-21: standard test method for transition temperatures and enthalpies of fusion and crystallization of polymers by differential scanning calorimetry. West Conshohocken, PA: ASTM International; 2021. p. 6. <http://dx.doi.org/10.1520/D3418-21>.
 35. ISO: International Organization for Standardization. ISO 13885-1:2020: Gel Permeation Chromatography (GPC) Part 1: Tetrahydrofuran (THF) as eluent. Geneva: ISO; 2020. p. 12.
 36. Tutak W, Sarkar S, Lin-Gibson S, Farooque TM, Jyotsnendu G, Wang D, et al. The support of bone marrow stromal cell differentiation by airbrushed nanofiber scaffolds. *Biomaterials*. 2013;34(10):2389-98. <http://dx.doi.org/10.1016/j.biomaterials.2012.12.020>.
 37. Zhang Z, Ji D, He H, Ramakrishna S. Electrospun ultrafine fibers for advanced face masks. *Mater Sci Eng Rep*. 2021;143:100594. <http://dx.doi.org/10.1016/j.mser.2020.100594>. PMID:33519094.
 38. Leith D, L'Orange C, Volckens J. Quantitative protection factors for common masks and face coverings. *Environ Sci Technol*. 2021;55(5):3136-43. <http://dx.doi.org/10.1021/acs.est.0c07291>. PMID:33601881.
 39. Abd Halim NS, Wirzal MD, Hizam SM, Bilad MR, Nordin NA, Sambudi NS, et al. Recent development on electrospun nanofiber membrane for produced water treatment: a review. *J Environ Chem Eng*. 2021;9(1):104613.
 40. Zander NE, Gillan M, Sweetser D. Recycled PET nanofibers for water filtration applications. *Materials (Basel)*. 2016;9(4):247.
 41. Sow PK, Singhal R. Sustainable approach to recycle waste polystyrene to high-value submicron fibers using solution blow spinning and application towards oil-water separation. *J Environ Chem Eng*. 2020;8(2):102786.
 42. Moon S, Farris RJ. The morphology, mechanical properties, and flammability of aligned electrospun polycarbonate (pc) nanofiber. *Polym Eng Sci*. 2008;48(9):1848-54. <http://dx.doi.org/10.1002/pen.21158>.
 43. Mubarak NM, Khalid M, Walvekar R, Numan A. *Contemporary nanomaterials in material engineering applications*. 1st ed. Switzerland: Springer; 2020.
 44. Thakur VK. *Nanostructured materials and their applications*. 1st ed. Singapore: Springer; 2021.
 45. Jang BN, Wilkie CA. A TGA/FTIR and mass spectral study on the thermal degradation of bisphenol a polycarbonate. *Polym Degrad Stabil*. 2004;86(3):419-30. <http://dx.doi.org/10.1016/j.polyimdegradstab.2004.05.009>.
 46. Feng J, Hao J, Du J, Yang R. Using TGA/FTIR TGA/MS and cone calorimetry to understand thermal degradation and flame retardancy mechanism of polycarbonate filled with solid bisphenol a bis(diphenyl phosphate) and montmorillonite. *Polym Degrad Stabil*. 2012;97(4):605-14. <http://dx.doi.org/10.1016/j.polyimdegradstab.2012.01.011>.
 47. Yilbas BS, Abubakar AA, Al-Qahtani H, Shuja SZ, Shaukat MM, Sahin AZ, et al. Solution crystallization of polycarbonate surfaces for hydrophobic state: water droplet dynamics and life cycle assessment towards self-cleaning applications. *Polymers (Basel)*. 2021;13(9):1449. <http://dx.doi.org/10.3390/polym13091449>. PMID:33946140.
 48. Yilbas BS, Ali H, Al-Aqeeli N, Khaled M, Abu-Dheir N, Varanasi KK. Solvent-induced crystallization of a polycarbonate surface and texture copying by polydimethylsiloxane for improved surface hydrophobicity. *J Appl Polym Sci*. 2016;133:43467. <http://dx.doi.org/10.1002/app.43467>.
 49. Aharoni SM, Murthy NS. Effects of solvent-induced crystallization on the amorphous phase of polycarbonate of bisphenol a. *Int J Polym Mater*. 1998;42(3-4):275-83. <http://dx.doi.org/10.1080/00914039808033875>.
 50. Moslan MS, Othman MHD, Samavati A, Salim MAM, Rahman MA, Ismail AF, et al. Fabrication of polycarbonate polymer optical fiber core via extrusion method: the role of temperature gradient and collector speed on its characteristics. *Opt Fiber Technol*. 2020;55:102162. <http://dx.doi.org/10.1016/j.yofte.2020.102162>.
 51. Uematsu H, Naganawa R, Higashitani N, Yamaguchi A, Yamane M, Ozaki Y, et al. Interfacial shear strength and interaction between polycarbonate and reinforcement fibers. *Polymer (Guildf)*. 2021;213:123301. <http://dx.doi.org/10.1016/j.polymer.2020.123301>.